Testing and analysis of cement foam materials for coal mine seals

K.M. Mohamed and R.K. Zipf, Jr.
Mining engineer and senior mining engineer, respectively, National Institute for Occupational Safety and Health, Office of Mine Safety and Health Research, Pittsburgh, PA, USA

Abstract

The shear strength properties of generic cement foam material and cement foam/concrete interfaces were examined at three testing scales. In laboratory direct shear tests on specimens with average shearing area of 0.006 m^2 (10 $in.^2$), the cement foam material had average peak and residual shear strengths of 0.88 MPa (128 psi) and 0.39 MPa (56 psi), respectively. Depending on the concrete strength, the cement foam/concrete interfaces had peak and residual shear strengths ranging from 0.71 to 0.81 MPa (103 to 117 psi) and from 0.27 to 0.29 MPa (39 to 42 psi), respectively. In laboratory direct double shear tests on specimens with average shearing area of 0.084 m^2 (130 $in.^2$), the cement foam/concrete interfaces had average peak and residual shear strengths of 0.17 to 0.30 MPa (25 to 44 psi) and of 0.11 to 0.23 MPa (16 to 33 psi), respectively. In large shear tests of simulated cement foam seals with the Mine Roof Simulator (MRS) test frame, cement foam/concrete interfaces with shearing area of 1.486 m^2 (2,304 $in.^2$) had average shear strengths of about 0.08 and 0.16 MPa (11 and 23 psi) along the roof and floor interfaces, respectively. The average shear strength through the cement foam material was 0.38 MPa (55.3 psi).

Finite element analysis of the large seal tests and the back analysis of the shear strength of full-scale cement foam seals conducted at the NIOSH Lake Lynn Laboratory confirmed shear strength of about 0.14 MPa (20 psi) along the seal/rock interfaces. The study concluded that the structural analysis of cement foam seals should be based on their residual shear strength determined from small laboratory-scale tests of the cement foam/concrete or rock interface and not be based on their peak strength.

Key words: Mine seal design, Cement foam seals, Mine seal testing, Numerical modeling, Mine seal resistance function

2014 *Transactions of the Society for Mining, Metallurgy & Exploration,* Vol. 336, pp. 467-482.

Introduction

Coal mine seals are structures built in underground coal mines to isolate abandoned mining areas from active mine workings. The current coal mine seal regulations (Final Rule, 2008) require seals to resist an explosion pressure of 0.83 MPa (120 psi) or more. Under the regulation, engineers must design the seals to resist one of four pressure-time curves, depending on the seal application. Seals made from cement foam make up a significant portion of new seals constructed in the U.S. coal industry under the new seal regulations.

Cement foam seals are made from a material similar to foamed concrete or cellular concrete. It can be made from Portland cement and water slurry to which foam is added. Cement foam contains no sand or aggregate; however, fly ash, fibers and other chemicals may be added to the mix to customize its mechanical properties (Dolton and Hannah, 2006). Cement foam is lightweight, free-flowing, non-toxic and non-combustible. It does not require compaction, is easy to pump, has excellent thermal insulating properties, and has energy-absorbing characteristics (Barnes, 2009).

Three distinct types of analysis methods can be used to design mine seals to resist a dynamic load such as a coal-mine explosion: equivalent static method, single-degree-of-freedom (SDOF) method, and numerical modeling methods (Mohamed et al., 2013).

The equivalent static method requires knowledge of the shear strength of the seal material, the surrounding rock and the interface. The critical input for the SDOF method is a resistance function for the seal that describes the frontal load-bearing capacity of the structure versus its center-point displacement (USACE, 2008; Slawson, 1995). A resistance function for a mine seal can be determined experimentally through the testing of structures or calculated using numerical modeling techniques. The resistance function of a mine seal depends on its geometry, construction materials, foundation strength and support conditions. Numerical modeling methods have the most extensive input requirements. Developing the needed input parameters for a numerical model can require laboratory testing and field evaluations.

The objective of this testing work is to develop the shear

Paper number TP-14-016. Original manuscript submitted August 2013. Revised manuscript accepted for publication March 2014. Discussion of this peer-reviewed and approved paper is invited and must be submitted to SME Publications Dept. prior to September 30, 2015.

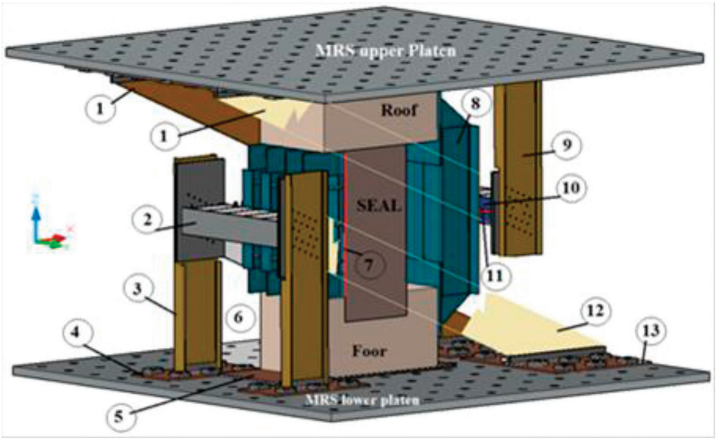

Reaction diagonal plate (24-in x 1-in)	5. Plate 13-mm (½-in) thick	9. Reaction support column W610x82 (WF24x55)	13. Diagonal shoe 25-mm (1-in) thick
2. Loading horizontal beam W610x155 (WF24x104)	6. Loading vertical beams W610x82 (WF24x55)	10. Reaction horizontal beam W610x155 (WF24x104)	14. Round bar 76-mm (3-in)-diameter
3. Loading support column W610x82 (WF24x55)	7. Loading plate 13-mm (0.5-in) thick	11. Round bar 50-mm (2-in)-diameter	
4. Column shoe 25-mm (1-in) thick	8. Reaction vertical beams W610x155 (WF24x104)	12. Loading diagonal plate 610-mmx 25-mm (24-in x1-in)	

Figure 1 — Isometric (left) and cross-sectional (right) illustrations of MRS seal testing fixture and seal model inside the MRS.

strength data, resistance functions and numerical modeling inputs necessary for the analysis of cement-foam coal mine seals. Development of this information required the extensive testing of cement foam and related materials on the laboratory scale and on a large scale using a special test fixture.

New large-scale testing method

Prior methods for the full-scale testing of coal mine seals used either an explosion test or a hydrostatic test (Weiss et al., 2002; Sapko et al., 2005, Weiss and Harteis, 2008). However, due to the closure of the underground test mine at the National Institute for Occupational Safety and Health (NIOSH)'s Lake Lynn Laboratory, these test methods became unavailable after 2008. Therefore, NIOSH researchers developed a new large-scale testing method for simulated coal mine seals based on the ASTM E72-02 method (ASTM, 2002). NIOSH researchers designed and built a large testing fixture with a loading capacity of 40 MN (900,000 lb) for use in the Mine Roof Simulator (MRS) loading frame located at the NIOSH Office of Mine Safety and Health Research, Pittsburgh, Pennsylvania (Zipf et al., 2009; Mohamed et al., 2013). The MRS approach provided a key vertical loading (convergence) element that was not possible with underground testing at the Lake Lynn mine.

Figure 1 shows an isometric drawing (on the left) of the seal testing fixture mounted in the MRS, and a cross-sectional view through the simulated test seal (on the right). The test fixture is composed of two similar opposing frames, one for load application and the other for reaction. The reaction (top) frame is stationary, while the loading (bottom) frame moves horizontally with the lower platen of the MRS. The main concept of the testing fixture is to use the MRS's vertical loading capability to apply a vertical load on the test seal to simulate roof-to-floor convergence, and its horizontal loading capability to apply uniform static load on the face of the test seal. With reference to Fig. 1, the loading and reaction frames include horizontal beams (parts 2 and 10) connected to support columns (parts 3 and 9) and diagonal plates (parts 1 and 12). The support columns and diagonals are welded onto 1-inch-thick steel plates (shoes—parts 4 and 13), which are fastened into the platens of the MRS using 70 high-strength 3-inch-diameter bolts. The vertical loading and reaction beams (parts 6 and 8) are hung from the horizontal loading and reaction beams (parts 2 and 10). The vertical loading and reaction beams can rotate freely around horizontal bars (parts 11 and 14, respectively).

The applied load on the face of the seal is developed by the horizontal actuators located under the lower platen of the MRS. This force is transferred to the horizontal and vertical loading beams via the diagonal loading plates on both sides of the seal model. The horizontal force is applied on the loading face of the seal via a stiffened 13-mm (0.5-in.)-thick loading plate (part 7). Rollers with diameter of 19 mm (¾ in.) are placed underneath the plate (part 5) and the floor block of the test model to ensure that the lower platen of the MRS slides under the model during horizontal movement of the lower platen. The vertical reaction beams constrain the horizontal displacement of the roof and floor blocks of the seal model. Hence, the applied horizontal load is transferred to the horizontal reaction beam and reaction diagonal plates.

Figure 2 shows the simulated seal test specimen, which

measures 1.83 m (6 ft) high by 1.22 m (4 ft) wide by 1.22 m (4 ft) thick, along with the two concrete foundation blocks—roof and floor—which measure 1.02 m (3.33 ft) high by 1.22 m (4 ft) wide by 2.03 m (6.67 ft) deep. Also shown are the loading vertical beams on the face of the test seal, and the reaction vertical beams on the face of the foundation blocks.

Load on the face of the simulated seal test specimen is derived from measurement of the horizontal ram pressure of the MRS. Any vertical load on the simulated seal test specimen is derived from measurement of the vertical ram pressure of the MRS.

The instrumentation system on the simulated seal test specimens shown in Fig. 2 measured the following:

- Horizontal displacement of the vertical reaction beam
- Horizontal displacement of the seal at mid-height
- Differential displacement between the cement foam seal and the concrete roof and floor foundations
- Upper-to-lower (roof-to-floor) displacement of the foundations
- Strain in critical members of the MRS seal testing fixture

Displacement measurements were made with linear position transducers (also known as string potentiometers or string pots) that were mounted onto a stationary reference frame fixed to the upper platen of the MRS, as shown in Fig. 2. This reference frame consisted of two vertical posts with a U-shaped horizontal bracket connecting the posts at mid-height of the seal.

Six string pots were mounted on each vertical post—three at the upper seal/roof interface and three at the lower seal/floor interface on the left and right side of the simulated seal test specimen. At each of these locations, the string pots measured displacements of the seal top or bottom, of the roof or floor block, and of the top or bottom of the reaction beam relative to the reference frame. From these absolute displacement measurements, relative horizontal motions of the seal and foundation blocks could be discerned.

Six string pots were also mounted on the horizontal bracket at seal mid-height—two each at the left side, center and right side of the bracket. At each of these locations, the string pots measured displacement of the seal midpoint and the reaction beam midpoint relative to the reaction frame. With these absolute displacement measurements at mid-height of the seal and the other horizontal displacement measurements at the seal/foundation block interfaces, bending motion of the seal could be discerned if it developed.

Two string pots were mounted between the upper and lower (roof and floor) foundation blocks. These displacement measurements identified the development of rotational movement of the foundation blocks and thus the development of arching action during the test.

Two strain gauges were mounted on each diagonal and two sets of strain gauges were also mounted on each loading and reaction horizontal beam. These gauges were monitored to ensure that (1) the seal test fixture remained within the linear elastic range of steel and (2) the loads were applied symmetrically and uniformly to the seal. Up to the moment of seal failure, the measured strain in the loading horizontal beam (part 2 in Fig. 1) was within 5% of that in the reaction horizontal beam (part 10 in Fig. 1). Similarly, the measured strain in the loading and reaction diagonals (parts 1 and 12 in Fig. 1) on both the left and right sides of the test frame agreed to within 5%. The uniformity of these measurements in the test fixture indicates that bending, racking or other anomalous, unwanted movement did not develop within the test seal. The test fixture performed as designed, and it delivered a uniform load across the test seal face up to the moment of seal failure.

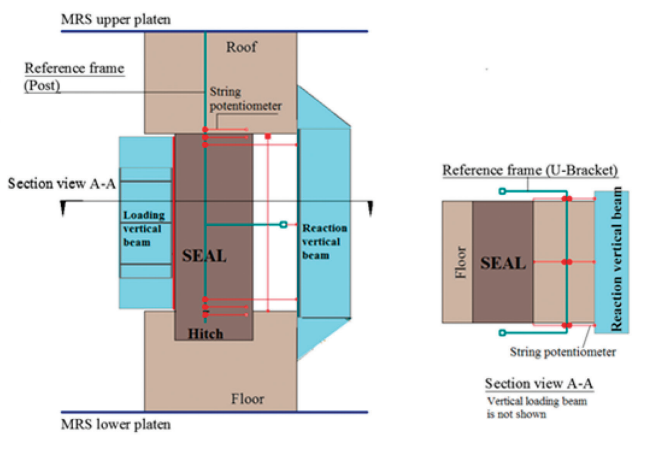

Figure 2 – Side-view (left) and top-view (right) illustrations of test specimen and MRS seal testing fixture showing displacement measurement system (not to scale).

The new large-scale testing method was first used on test specimens made of reinforced concrete and plain concrete (Mohamed et al., 2013). Test results using those materials demonstrated the reliability and reproducibility of this new test method. The loading frame in the MRS delivered uniform load to the test seal face, and the loads and the reactions were symmetric. No extraneous shear loads or bending moments were imparted to the simulated seal test specimen.

Seal model construction began by pouring the concrete roof and floor foundation blocks. Following a cure period, the foundation blocks were assembled into a steel frame, and formwork was built between the concrete roof and floor foundation blocks. Polypropylene rope (3/8-inch-diameter) on 2-ft-centers connected opposite faces of the formwork to support it while pouring the wet cement foam. The inner surfaces of the formwork were lined with 6-mil plastic film to contain the wet cement foam and to prevent water loss during the 28-day curing period.

Cement foam for the simulated seals was pumped into the form in one continuous pour lasting about five hours. Pumping continued until the cement foam material reached the roof and made contact all around the upper seal perimeter. Visual observation of the cement foam/concrete roof block contact indicated that full contact between the two materials was achieved at this interface.

Design and testing of generic cement foam material

Cement foam for this study was made by first creating a well-mixed slurry of ordinary Portland cement (Type I/II) and potable water. This slurry was "neat," meaning it contained no sand, aggregate or other additives. Stable foam was made using a commercial foam generator (Cretefoamer) and a synthetic surfactant (Cretefoamer CMX) (Richway Industries, 2013). Foam was added to the cement-water slurry, followed by mixing until the cement foam density was 961 kg/m^3 (60 pcf).

Specifications of the generic cement foam are summarized

Table 1 — Mixture design and properties of cement foam seal material and concrete roof and floor blocks.

Specifications	Cement foam for seal	Concrete for roof block	Concrete for strong floor block	Concrete for weak floor block
Water-cement ratio	0.5	0.35	0.45	1.64
Cement / sand / aggregate ratio	n.a.	1/2.5/3.6	1/1.2/3.1	1/11/12
Wet and dry densities, kg/m^3 (pcf)	961 and 897 (60 and 56)			
Foam density, kg/m^3 (pcf)	48 (3)		not applicable	
Porosity, %	52			
Number of tests	38	2	4	3
Unconfined compressive strength Average and standard deviation MPa (psi)	3.10 (449) ± 0.88 (128)	24.10 (3,495) not applicable	40.03 (5,804) ±2.43 (352)	1.54 (224) ±0.05 (7)
Young's modulus Average and standard deviation MPa (psi)	979.31 (142,000) ±268.97 (39,000)	7,655.17 (1,110,000) not applicable	10,068.97 (1,460,000) ±282.76 (41,000)	648.28 (94,000) ±13.79 (2,000)

Table 2 — Summary of direct shear test results, average and standard deviation, on 0.006-m^2 (10-in.^{2}) specimens of cement foam and cement foam/concrete interfaces.

Test type	No. of tests	Peak shear strength – MPa (psi) average and standard deviation	Residual shear strength – MPa (psi) average and standard deviation	Shear stiffness – MPa/m (psi/in.) average and standard deviation
Cement foam	7	0.88 ± 0.10 (128 ± 14)	0.39 ± 0.11 (56 ± 16)	1,906 ± 1,104 (7,020 ± 4,068)
Cement foam/concrete roof block interface	6	0.81 ± 0.12 (117 ± 18)	0.28 ± .08 (40 ± 12)	1,144 ± 203 (4,215 ± 750)
Cement foam/concrete strong floor block interface	6	0.80 ± 0.25 (116 ± 36)	0.29 ± 0.15 (42 ± 22)	997 ± 157 (3,673 ± 577)
Cement foam/concrete weak floor block interface	3	0.71 ± 0.09 (103 ± 13)	0.27± 0.10 (39 ± 14)	1,448 ± 219 (5,333 ± 808)

in Table 1, along with specifications of the concrete used for the roof and floor blocks in the simulated seal test specimens. Test specimens of the cement foam and the roof and floor concrete were protected with plastic wrap to prevent excessive moisture loss and cured at room temperature for a minimum of 28 days in conditions similar to the simulated seal test specimens. Unconfined compressive strength tests and Young's modulus measurements were performed on numerous laboratory test specimens of the cement foam and concrete, and these test results are also summarized in Table 1.

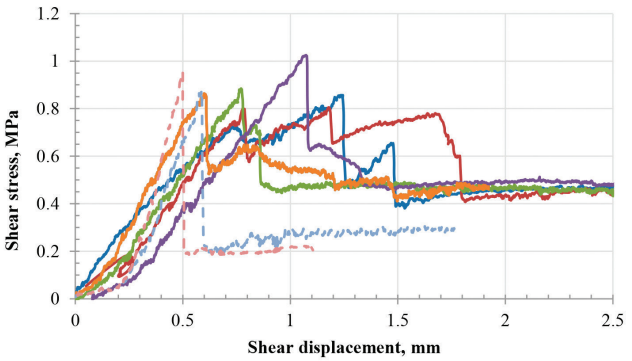

Figure 3 — Shear stress-displacement curves for seven direct shear tests of cement foam material (dashed lines are cylindrical specimens).

Direct shear tests with cement foam on small specimens

Direct shear experiments were performed on two different sizes of small test specimens. About half the specimens were cylinders with diameter of 102 mm (4 in.) and shear area of 0.008 m^2 (12.6 in.^{2}), and the other half were rectangular prisms with length of 76 mm (3 in.) and shear area of 0.006 m^2 (9 in.^{2}). Four types of direct shear specimens were prepared: cement foam over roof concrete, cement foam over strong floor concrete, cement foam over weak floor concrete, and intact cement foam. With the cement-foam-over-concrete specimens, the concrete was cured first and then the cement foam was poured. The interface was considered a kind of "cold joint." The cement-foam-direct-shear specimens were

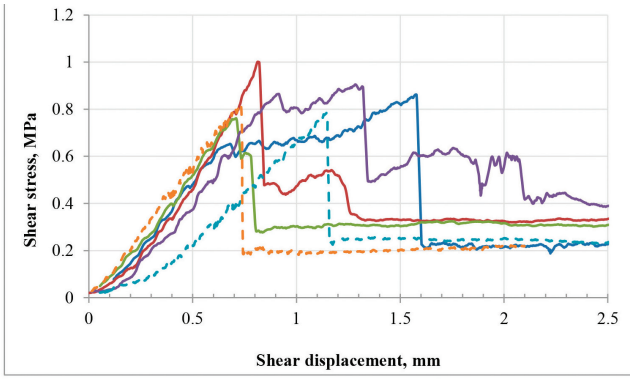

A. Cement foam / concrete roof block interface.

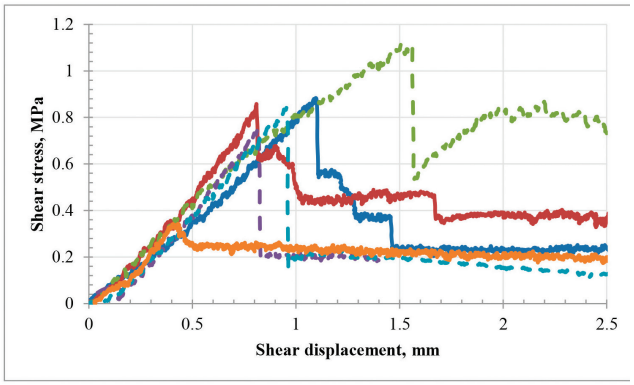

B. Cement foam / concrete strong floor block interface.

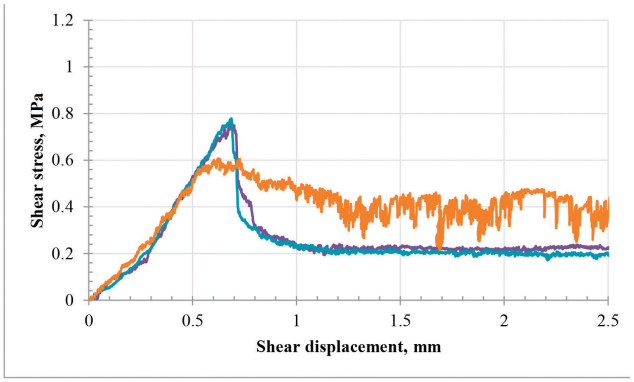

C. Cement foam / concrete weak floor block interface.

Figure 4 — Shear stress-displacement curves from direct shear tests along cement foam/concrete interfaces (dashed lines are cylindrical specimens).

poured all at once and therefore no cold joint existed. The direct shear test was through the cement foam material itself.

Figures 3 and 4 show the measured shear stress versus displacement for shear strength tests of the cement foam material and various cement foam/concrete block interfaces. In all cases, the shear strength exhibits elastic-brittle behavior with a peak shear strength and a lower residual shear strength. Table 2 summarizes the peak and residual shear strengths plus the shear stiffness from all direct shear tests on the small laboratory-scale specimens, which have an average shear area of about 0.006 m^2 (10 $in.^2$).

With the small laboratory-scale testing, the bond across each concrete/cement foam interface was ideal. All test specimens were protected with plastic wrap to prevent moisture loss and cured at room temperature for a minimum of 28 days prior to testing. None of these small test specimens became

Figure 5 — Photograph of double direct shear test fixture for 0.084-m^2 (130-$in.^2$) test specimens in test machine showing cement foam material loaded by ram and concrete roof and floor blocks.

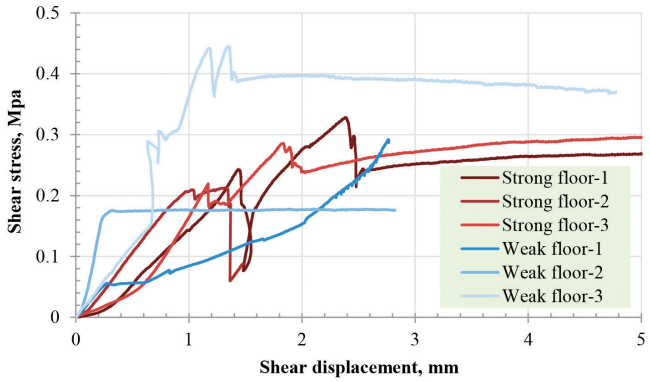

Figure 6 — Shear stress-displacement curves for double direct shear tests along cement foam/concrete block interfaces with 0.084-m^2 (130-$in.^2$) test specimens.

warm to the touch due to cement hydration during the initial curing period.

Direct shear tests with cement foam on 0.084-m^2 (130-$in.^2$) specimens

In addition to the small laboratory-scale direct shear tests, several direct shear tests were conducted on larger double direct shear specimens with two interfaces consisting of roof concrete/cement foam, and floor concrete/cement foam. The test fixture in the testing machine is shown in Fig. 5. The left side of the specimen is roof concrete; the right side is either strong or weak floor concrete, and the center is cement foam. The cement foam is loaded at the top by the loading machine and the concrete blocks on either side provide a reaction. Each test specimen is about 330 mm (13 in.) high and 254 mm (10 in.) wide and has a surface area of 0.084 m^2 (130 $in.^2$).

Figure 6 shows the shear stress-displacement curves for the six tests performed with this set-up. With the concrete roof block/cement foam/concrete strong floor specimens,

Table 3 — Summary of direct shear test results on 0.084-m^2 (130-$in.^2$) specimens of cement foam/floor concrete interfaces.

Test type	No. of data points	Peak shear strength – MPa (psi) average only	Residual shear strength – MPa (psi) average only	Shear stiffness – MPa/m (psi/in) average only
Cement foam/concrete roof block interface	6	0.17 (25)	0.11 (16)	about 190 (700)
Cement foam/concrete strong floor block interface	3	0.30 (44)	0.23 (33)	about 190 (700)

failure occurred first along the concrete roof block/cement foam interface. The shear stress along this interface first or initially decreased and then increased until failure occurred along the concrete strong floor/cement foam interface. With the concrete roof block/cement foam/concrete weak floor specimens, there was no bonding along the cement foam/concrete weak floor interface. Ideal bonding occurs when the concrete is saturated but the surface is dry. The weak concrete will be much more porous; therefore, it may have been more saturated and may have affected the bond by introducing water at the interface. With a high water-to-cement ratio, there is a lot of extra water in the material and if sealed, the water remains in the porous material as in a saturated sponge; if the material is dry, it will absorb water from the foam and weaken the foam. Failure occurred when the concrete roof block/cement foam interface ruptured.

As summarized in Table 3, these six tests with shear area of 0.084 m^2 (130 $in.^2$) provided six observations of the cement foam/concrete roof block peak and residual shear strengths, along with three observations of the cement foam/concrete strong floor block peak and residual shear strengths. With these larger laboratory-scale test specimens, the bond across each concrete/cement foam interface was also perfect; however, the cement foam/concrete weak floor interface did not have measureable shear strength. All test specimens were protected with plastic wrap and cured at room temperature for a minimum of 28 days prior to testing. None of these larger test specimens became warm to the touch due to cement hydration during the initial curing period.

Large-scale tests of cement foam seals in MRS

Eight tests of simulated cement foam seals were conducted using the new large-scale MRS testing method described earlier. The test program considered three variables—the floor anchorage condition, the presence or absence of vertical load on the simulated seal, and the strength of the floor material. The concrete floor block either contained a hitch to anchor the seal (H), as shown in Fig. 2, or it did not (NH), in which case, the anchorage solely relied on the shear strength of the interface between the cement foam/concrete foundation block only. The simulated seal either had a "conver-

Table 4 — Summary of large cement foam seal test results in MRS. The shear area is 1.486 m^2 (2,304 $in.^2$) for both upper and lower interfaces.

Test specimen designation	Face pressure at failure along cement foam/concrete roof block interface – MPa (psi) (circles in Figs. 7 and 8)	Average shear stress at failure along cement foam/concrete roof block interface – MPa (psi)	Face pressure at failure along cement foam/concrete floor block interface – MPa (psi) (non-hitched seals only) (squares in Fig. 7)	Shear stress at failure along cement foam/concrete floor block interface – MPa (psi) (non-hitched seals only)	Face pressure at failure through cement foam near floor block – MPa (psi) (hitched seals only) (triangles in Fig. 8)	Shear stress at failure through cement foam near floor block – MPa (psi) (hitched seals only)
#1 – NH_NC_S	0.08 (11)	0.06 (8.3)	0.14 (21)	0.16 (23.3)	-	-
#2 – NH_C_S	0.20 (29)	0.15 (21.8)	0.25 (36)	0.22 (32.3)	-	-
#3 – NH_NC_W	0.09 (13)	0.07 (9.8)	0.14 (21)	0.15 (21.8)	-	-
#4 – NH_C_W	0.17 (24)	0.12 (18)	0.21 (31)	0.20 (28.5)	-	-
#5 – H_NC_S	0.14 (20)	0.10 (15)	-	-	0.33 (48)	0.39 (57)
#6 – H_C_S	0.28 (40)	0.21 (30)	-	-	0.39 (56)	0.37 (54)
#7 – H_NC_W	0.09 (13)	0.07 (9.8)	-	-	0.31 (45)	0.40 (57.8)
#8 – H_C_W	0.14 (20)	0.10 (15)	-	-	0.31 (45)	0.36 (52.5)

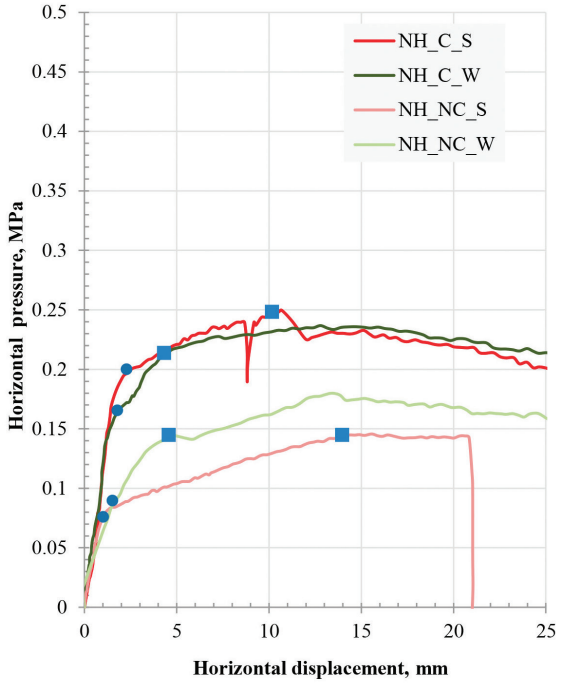

Figure 7 — Applied pressure on seal face versus horizontal displacement for non-hitched cement foam seal tests. (Circles: shear failure along cement foam/concrete roof block interface occurs; squares: shear failure along cement foam/concrete floor block interface occurs.)

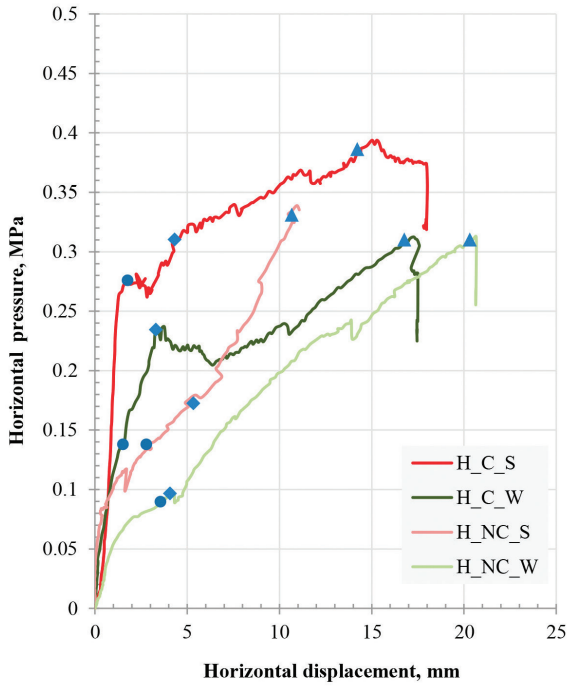

Figure 8 — Applied pressure on seal face versus horizontal displacement for hitched cement foam seal tests. (Circles: shear failure along cement foam/concrete roof block interface occurs; diamonds: shear failure through cement foam initiates near concrete floor block; triangles: final shear rupture through cement foam.)

gence" applied to the entire seal test specimen (C), or it did not (NC). Convergence in mining terminology corresponds to decreased distance between the surrounding roof and floor rocks due to mining-induced stress and rock creep. To simulate the effect of convergence in these experiments, the simulated seal either had a vertical load applied (C), or it did not (NC). Concrete in the lower block of the simulated seal test specimen shown in Fig. 2 was either strong floor concrete (S) or weak floor concrete (W) with the properties indicated in Table 1.

The nomenclature used in this study for the floor anchorage (hitching or non-hitching), vertical load or convergence (with or without vertical load or convergence), and block strength (strong or weak concrete for the floor) are H, NH, C, NC, S and W, respectively. As an example, a hitched seal without roof-to-floor convergence built on a strong floor is abbreviated as H_NC_S.

The MRS was operated in displacement control mode to apply loads to the simulated seal test specimens. If the simulated seal test had "convergence" applied, the vertical loading rams of the MRS were displaced a certain distance until the desired vertical load was achieved. For the "convergence" (C) seal tests, the vertical preload is equivalent to a vertical stress of 0.24 MPa (35 psi) in the simulated seals. The "non-convergence" (NC) tests also had a load equivalent to a vertical stress of 0.03 MPa (5 psi). Once the desired load was achieved on the seal test specimen, the displacement of the vertical ram was held constant during the remainder of the test. Pressure on the seal face was applied through the horizontal rams of the MRS moving in displacement control mode at a rate of 1 mm (0.025 in.) per minute. At this displacement rate, typical tests required about 110 minutes to complete.

Photographs were taken at 1-minute intervals during each test on both sides of the seal test specimen. These photographs showed the cement foam seal and the interfaces with the concrete roof and floor blocks. Paper strips with a 51-mm (2-in.) grid were glued to the cement foam and concrete blocks on each side of an interface to enhance the visibility of motion along the interface. The photographic record could be correlated to the pressure and displacement data acquired during the test for diagnosis of the failure mechanics.

Essential test data from the eight tests on simulated cement foam seals are summarized in Figs. 7-9 and Table 4.

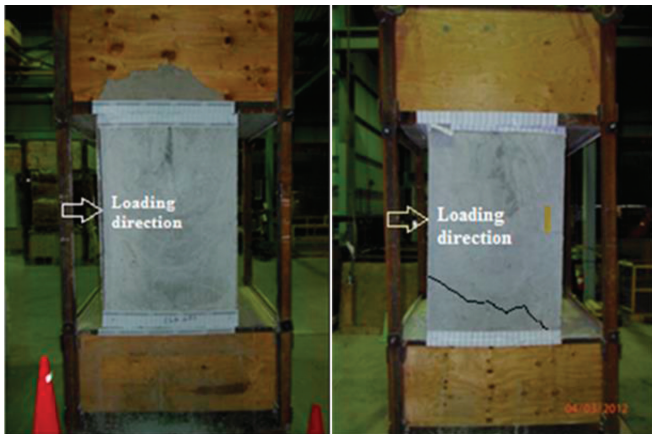

Figure 9 — Typical failure modes for cement foam seal tests. With non-hitched seals (left), shear failure occurred first along the cement foam/concrete roof block interface and then along the cement foam/concrete floor block interface. With hitched seals (right), shear failure occurred first along the cement foam/concrete roof block interface and then through the cement foam material near the concrete floor block.

Figure 7 for the four non-hitched (NH) seal tests and Fig. 8 for the four hitched (H) seal tests show the applied pressure on the seal face versus the horizontal displacement at the mid-height of the seal. The applied pressure on the seal face is calculated from the horizontal ram pressure in the MRS measured during the test. The horizontal displacement is calculated by averaging displacement measurements on the left side, center and right side of the seal at mid-height. Figure 9 shows two seals after testing to failure that illustrate the two different failure modes that developed during the tests. With non-hitched seals (left), shear failure occurred first along the cement foam seal/concrete roof block interface and then along the cement foam seal/concrete floor block interface. With hitched seals (right), shear failure also occurred first along the cement foam seal/concrete roof block interface, but then cracking developed in the cement foam near the floor foundation block that ultimately led to shear rupture through the cement foam near the floor block.

From the four tests on non-hitched seals (Fig. 7), four stages of loading and failure development are observed:

1. Initial loading: In this stage, the seal is undergoing linear elastic deformation. No relative displacement is observed or measured along the cement foam/concrete block interfaces.
2. Cement foam/concrete roof block interface failure: Relative displacement is observed and measured along the cement foam/concrete roof block interface. This point is indicated by a circle in Fig. 7. The applied pressure versus horizontal displacement curve shown in Fig. 7 departs from linearity.
3. Cement foam/concrete floor block interface failure: Relative displacement is observed and measured along the cement foam/concrete floor block interface. This point is indicated by a square in Fig. 7. The applied pressure on the seal face in Fig. 7 has reached a maximum.
4. Plastic deformation on both interfaces: In this stage, relative displacement along the cement foam/concrete block interfaces occurs at constant applied pressure on the seal face.

From the four tests on hitched seals (Fig. 8), four similar stages of loading and failure development are observed:

1. Initial loading: The seal undergoes linear elastic deformation. No relative displacement is observed or measured along the cement foam/concrete block interfaces.
2. Cement foam/concrete roof block interface failure: Relative displacement is observed and measured along the cement foam/concrete roof block interface. This point is indicated by a circle in Fig. 8. The applied pressure versus horizontal displacement curve shown in Fig. 8 departs from linearity.
3. Shear failure initiation through the cement foam seal near the concrete floor block: A crack is observed in the cement foam near the concrete floor block opposite the loaded face. This point is indicated by a diamond in Fig. 8.The applied pressure versus horizontal displacement curve shown in Fig. 8 usually changes slope.
4. Violent shear rupture through the cement foam seal near the concrete floor block: At this stage, the shear strength of the cement foam is exceeded. This point is indicated by a triangle in Fig. 8. The applied pressure on the seal face and the shear strength of the seal usually decrease significantly at this point.

Table 4 summarizes the key failure information extracted from the eight large-scale tests on simulated cement foam seals conducted in the MRS. From the applied pressure to the seal face at which failure along the cement foam/concrete roof block interface develops (circle points in Figs. 7 and 8), the shear stress at failure along the roof interface is computed by:

$$C_{roof} = \frac{P_{face} \times H}{(2t)} \quad (1)$$

where P_{face} is the applied pressure on the seal face, H is the seal height, and t is the seal thickness.

From the applied pressure to the seal face at which failure along the cement foam/concrete floor block interface develops (square points in Fig. 7), the shear stress at failure along the floor interface, C_{floor}, is computed by:

$$C_{floor\ or\ cement\ foam} = \frac{P_{face} \times H}{t} - C_{roof} \quad (2)$$

From the applied pressure to the seal face at which failure through the cement foam develops (triangle points in Fig. 8), the shear stress at failure through the cement foam, $C_{cement\ foam}$, is also computed by Eq. (2).

From the data presented in Table 4, the following observations were made about the large-scale tests of cement foam seals in the MRS:

1. Failure occurred first along the upper interface between the cement foam and the concrete roof block, and then along the lower interface at the concrete floor block in the case of non-hitched test seals or through the cement foam material near the floor in the case of hitched test seals. This observed failure sequence reflects the construction process since the simulated cement foam seal was built from floor to roof. A better bond and higher shear strength are expected between the cement foam/concrete floor block than between the cement foam/concrete roof block.
2. Average shear strength along the cement foam/concrete roof block interface is 0.1 MPa (14.5 psi) for the non-hitched tests and 0.12 MPa (17.5 psi) for the hitched tests. As expected, these values are similar, since the floor condition—hitched or non-hitched and strong or weak—should have no effect on the strength of the upper interface between the cement foam and concrete roof block.
3. A vertical load to simulate roof-to-floor convergence increases the shear strength of the cement foam/concrete roof block interface. All "C" test specimens have greater shear strength than their corresponding "NC" test specimens.
4. From the non-hitched tests, average shear strength along the cement foam/concrete floor block interface is 0.18 MPa (26.5 psi). The strength of the concrete floor block may increase the shear strength of the lower interface. The two strong floor concrete foundation tests had greater shear strength than the two weak floor concrete foundation tests. However, this initial observation may not be statistically significant.

Cement foam / concrete roof block interface. | Cement foam / concrete strong floor block interface. | Cement foam / concrete weak floor block interface.

Figure 10 — Photographs of de-bonding at cement foam/concrete block interfaces after testing.

5. With the non-hitched test specimens, a vertical load to simulate roof-to-floor convergence increases the shear strength of the cement foam/concrete floor block interface. All "C" test specimens have greater shear strength than their corresponding "NC" test specimens.
6. Average shear strength through the cement foam material derived from the hitched tests is 0.38 MPa (55.3 psi). This value appears to be unaffected by the application of a vertical load to simulate roof-to-floor convergence.

Data from this series of eight tests of simulated cement foam seals indicate that the test method performed similarly to earlier test series with reinforced concrete and plain concrete (Mohamed et al., 2013). The loading frame in the MRS delivered a uniform and symmetric load to the test seal face. Observations of shear strength derived from the test matrix are logical and expected. The observed failure modes are sensible. Failure occurs first at the upper interface and then either along the lower interface or through the cement foam material low in the test specimen.

After testing, the concrete roof block/cement foam seal/concrete floor block assemblies were carefully disassembled, and the upper and lower interfaces were observed. Figure 10 shows typical photographs of these surfaces. In all cases, debonding between the cement foam and the concrete is evident.

The eight large-scale tests on simulated cement foam seals may have been affected by heat generated by cement hydration during the seal curing. About five hours after pumping the cement foam test seals, the formwork became warm to the touch with temperature estimated at 339K (150°F), and steam emanated from the curing cement foam at the polypropylene ropes. By the next morning, the steam emanations had ceased, but the test seals remained warm at about 311K (100°F) for several more days. Jones and McCarthy (2006) presented a method to estimate the temperature inside a concrete block due to cement hydration. For a 1.22-m (4-ft)-wide by 1.83-m (6-ft)-high by 1.22-m (4-ft)-thick block containing about 1,562 kg (3,500 lb) of Portland cement, the expected internal temperature is about 465K (377°F). This estimated internal temperature is consistent with the observed external temperature. Following a 28-day minimum cure period, the formwork and plastic film liner were removed prior to testing. After careful inspection, no cracks or other defects were observed in the test seals. The possibility exists that the high internal curing temperature adversely affected the mechanical properties of the test seal, but for reasons discussed later, the effect is negligible or small.

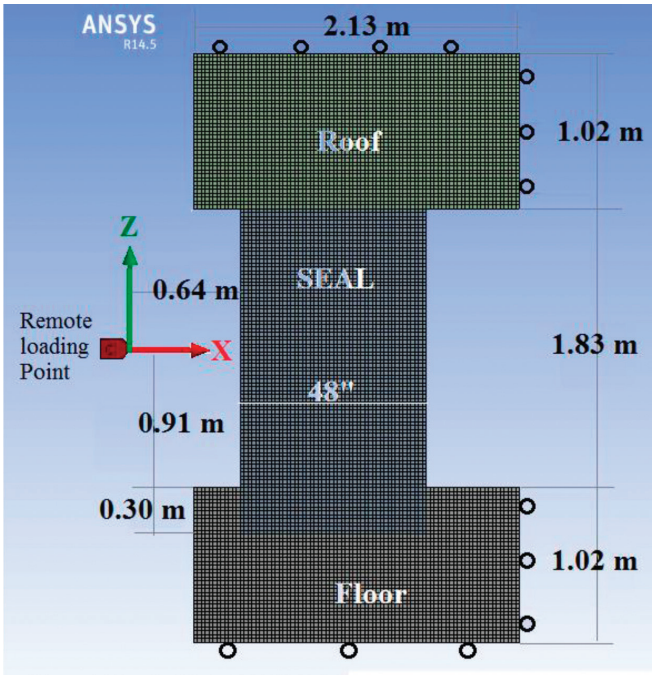

Figure 11 — FE model of cement foam test seal and concrete roof and floor blocks.

Finite element analysis of cement foam seal tests in MRS

ANSYS Version 14.5 was used to simulate the static load-displacement response of the test seals in the MRS. Figure 11 shows a typical model of the test arrangement. The model is two-dimensional, and the plane stress assumption is used. Element sizes in this model are about 51 mm (2 in.). Rollers were used to simulate the interaction of the concrete roof and floor blocks with the upper and lower steel platens of the MRS. Rollers were also used to simulate the reactions of the MRS test frame against the upper and lower blocks.

The displacement approach was used to apply load to the test seal face in the model. This approach enabled simulation of the test seal up to and beyond failure without numerical instability in the model. As shown in Fig. 11, a remote loading point was created that reflects the round bar on the horizontal loading beam (parts 2 and 6, Fig. 1). This point, located about 635 mm (25 in.) from the seal face, is coupled to all points along the test seal face. The point is then displaced horizontally to induce load on the test seal face. Rotation is allowed about this point to ensure that zero moment is applied. Model loading occurs in two steps: (1) the lower floor block is displaced vertically in the z-direction to induce the desired vertical load, which simulates roof-to-floor convergence, and (2) the remote loading point is displaced horizontally to induce load on the seal face.

The finite element analysis model is constructed from three major elements: (1) a concrete material model, (2) a cement foam material model, and (3) an interface model. In its element library, ANSYS Version 14.5 includes "Solid65," which is a version of the William-Warnke model for plain concrete. The original William-Warnke model (Hauksdóttir, 2007) is a triaxial failure surface in principal stress space to define the onset of cracking and crushing in plain concrete. The ANSYS 14.5 implementation of this model also includes an isotropic, work-hardening stress-strain relationship and the Von Mises and Drucker-Prager failure criteria. These criteria define the onset of plastic deformation and shear failure

Table 5 — Summary of mechanical properties for various materials used in FE models.

Property		Cement foam for seal	Concrete for roof block	Concrete for strong floor block	Concrete for weak floor block
Young's modulus – MPa (psi)		275.86 (40,000)	7,655.17 (1,110,000)	10,068.97 (1,460,000)	648.28 (94,000)
Poisson's ratio		0.2	0.3	0.3	0.3
Compressive strength – MPa (psi)		3.10 (449)	24.10 (3,495)	40.03 (5,804)	1.54 (224)
Tensile strength – MPa (psi)		0.38 (55)	3.06 (443)	3.94 (571)	0.77 (112)
Cohesion – MPa (psi)		0.38 (55)	-	-	-
Friction angle, deg.		8	not applicable		
Cement foam/concrete interfaces	Friction coefficient	not applicable	0.5	0.5	0.2
	Cohesion – MPa (psi)		0.08 (12)	0.15 (22)	0.15 (22)
	Shear stiffness – MPa/m (psi/in)		61.3 (226)	61.3 (226)	61.3 (226)

in the material.

For the plain concrete blocks, the finite element analysis used the William-Warnke concrete model (Solid 65) with the von Mises failure criteria (Kachlakev et al., 2001; Vasudevan and Kothandaraman, 2011; Wolanski, 2004). The essential properties to specify for the material are its compressive and tensile strengths. For the cement foam seal, the analysis also used the William-Warnke concrete model (Solid 65), but with the Drucker-Prager failure criteria (Lee et al., 2004; Krieg, 1972). The properties specified are the compressive strength, tensile strength, cohesion, and friction angle of the cement foam material.

The Coulomb friction model was used to simulate the cement foam/concrete foundation block interfaces. The Coulomb friction model for interfaces is defined as (ANSYS 14.5):

$$F_{lim} = c_o \times A + \mu \times F_n$$

$$|\mathrm{F_s}| \leq \mathrm{F_{lim}}$$

where

F_s is the equivalent tangential force
F_n is the normal force in the interface
F_{lim} is the limiting frictional force
μ is the coefficient of friction
c_o is the cohesion
A is the shearing area

If the equivalent tangential force F_s is less than F_{lim}, the state is known as the sticking state. For F_s greater than F_{lim}, sliding occurs, and the state is known as the sliding state. The sticking/sliding calculations determine when a point transitions from sticking to sliding or vice versa.

The material properties used in these finite element analyses are summarized in Table 5. Young's modulus in the model for the concrete roof and floor blocks is the same as that measured in the laboratory reported in Table 1. The Young's modulus for the cement foam is back-calculated directly from the eight large-scale tests in the MRS. During the initial test stage, the seal behaves as a simply supported, uniformly loaded, linear-elastic beam with span of 1.83 m (6 ft). At a face load of 0.03 MPa (5 psi), the mid-point of this beam deflected 0.01 in., and Young's modulus is back-calculated as about 275.86 MPa (40,000 psi). This value is about 28% of the laboratory value reported in Table 1. The difference in Young's modulus between the laboratory tests and the large-scale tests in the MRS might be attributable to the heating of the cement foam seal reported earlier (Othuman and Wang, 2010). This heating phenomenon did not occur in the laboratory-scale test specimens, which may lead to higher values. Poisson's ratio is assumed to be 0.2 for the cement foam (Lee et al., 2004) and 0.3 for the concrete roof and floor blocks (Vasudevan and Kothandaraman, 2011; Wolanski, 2004).

The compressive strengths of the cement foam and concrete roof and floor block material are derived from laboratory tests, and those values reported in Table 1 are used in the model directly. The tensile strength of concrete can be estimated from its compressive strength with the following equation (Chen, 2007):

$$f_t = 7.5 * \sqrt{f_c'} \qquad (3)$$

where f_c' is the compressive strength.

The average shear strength through the cement foam material derived from the hitched tests is 0.38 MPa (55.3 psi). This value is approximately the same as the cohesion for the material. The tensile strength of the cement foam is assumed to equal its cohesion to reduce model instability.

Ehrgott (1973) conducted extensive triaxial compression tests on a cement foam material that is very similar to that used in this study. The dry density of Ehrgott's material was 657 kg/m^3 (41 pcf), and he measured a friction angle of 9.6° for the material. Lee et al. (2004) conducted compression and tension tests on cement foam with density of 961 and 1,442 kg/m^3 (60 and 90 pcf). The friction angle for both materials is 8.5°. Based on this data, a friction angle of 8° was assumed for the cement foam in this study.

Finite element analysis was conducted on each cement foam seal test for comparison with the corresponding large-scale tests in the MRS. All the analyses used the same material properties summarized in Table 5. Only the boundary conditions (hitching and convergence) on the model changed

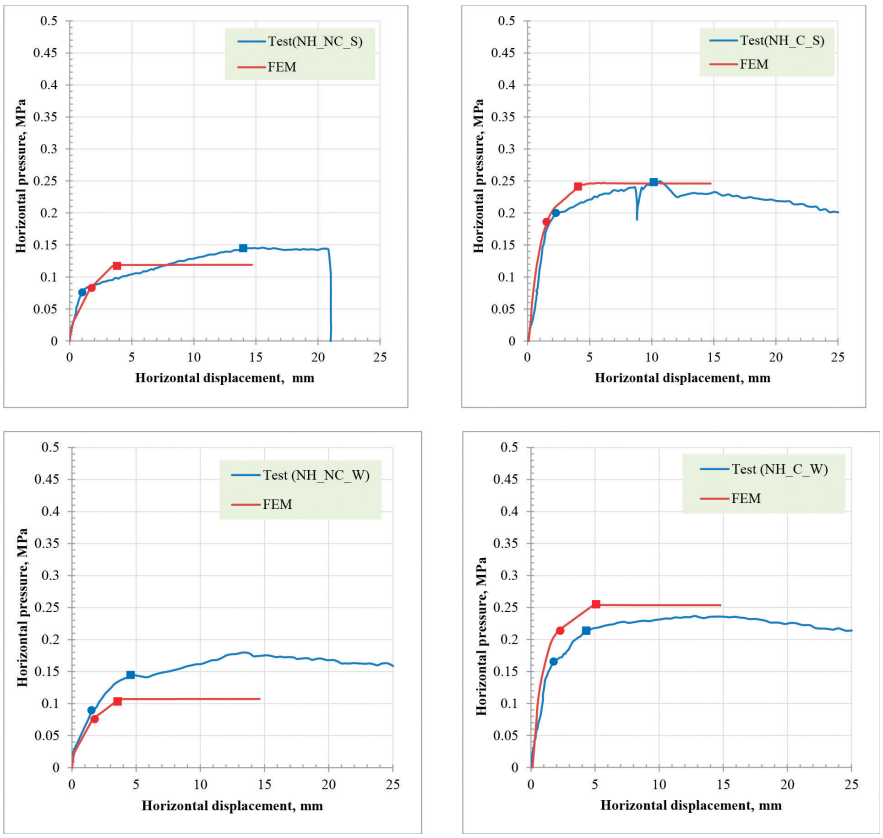

Figure 12 — Measured (blue) and predicted (red) horizontal face pressure versus displacement curves for non-hitched cement foam seal tests. (Circles: shear failure along cement foam/concrete roof block interface occurs; squares: shear failure along cement foam/concrete floor block interface occurs.)

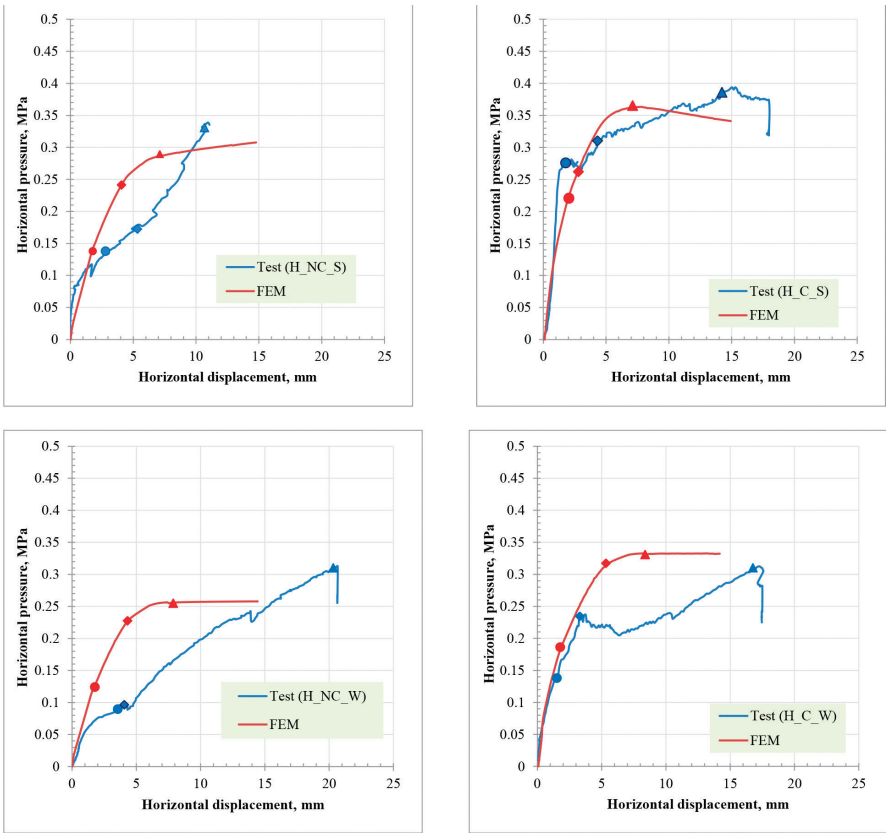

Figure 13 — Measured (blue) and predicted (red) horizontal face pressure versus displacement curves for hitched cement foam seal tests. (Circles: shear failure along cement foam/concrete roof block interface occurs; diamonds: shear failure through cement foam initiates near concrete floor block; triangles: final shear rupture through cement foam.)

to simulate the actual test conditions.

The comparison between the finite element analysis and the test measurements considered the following conditions: (1) failure pattern and sequence (2) horizontal pressure and displacement at critical loading stages, and (3) shape of the horizontal pressure versus displacement curve. Figures 12 and 13 show the calculated horizontal face pressure on the test model versus the calculated horizontal displacement at mid-height of the test seal for the non-hitched tests and the hitched tests. For comparison with the calculations, the measured test data shown in Figs. 7 and 8 are repeated.

With both the non-hitched and hitched calculations, the finite element analyses confirmed the same failure patterns and sequences observed during the large-scale tests in the MRS. For the non-hitched seal models, the finite element analyses first indicated failure at the cement foam/concrete roof block interface followed by failure at the cement foam/concrete floor block interface. The model calculations show no yielding or cracking within the cement foam seal itself. The calculated magnitude of horizontal face pressure at which shear failure occurs along the cement foam/concrete roof block interface (circle points) and along the cement foam/concrete floor block interface (square points) agree well in all cases with the large-scale tests in the MRS. The calculated magnitude of horizontal displacement at which shear failure developed agreed well with the experiment along the cement foam/concrete roof block interface, but was generally too small along the cement foam/concrete floor block interface. Most important is the general shape of the calculated horizontal pressure versus horizontal displacement curve compared with the experiment. As shown in Fig. 12, the calculated curve matches the measured curve well for all four experiments. In particular, the calculated horizontal pressure at which constant plastic deformation occurs along both interfaces (roof and floor) agrees well with experimental observation.

For the hitched seal models, the finite element analyses first indicated failure at the cement foam/concrete roof block interface followed by rupture through the cement foam material near the floor. The analyses calculated well the magnitude of the horizontal face pressure at which shear failure along the cement foam/concrete roof block interface occurred (circle points), and the pressure magnitude at which final shear rupture occurred through the cement foam material (square points). However, the magnitude at which shear failure through the cement foam material initiated (diamond points) was not calculated as well. The general shape of the calculated horizontal pressure versus horizontal displacement curve for the hitched experiments matches the measured curves well, as shown in Fig. 13, except for the H_NC_W test.

Shear strengths of cement foam and interfaces at different scales

The testing in this study developed shear strength data for a generic cement foam material at three different scales with shearing areas of about 0.006, 0.084 and 1.486 m^2 (10, 130 and 2,304 $in.^2$). Table 6 summarizes the measured peak and residual shear strengths for the cement foam material and the interfaces between cement foam and concrete. The data for the tests for areas of 0.006, 0.084 and 1.486 m^2 (10, 130 and 2,304 $in.^2$) in this table are extracted from Tables 2, 3 and 4, respectively. The peak and residual shear strengths versus shearing area data in Table 6 is shown in Fig. 14. Small shearing area test specimens exhibit a distinct peak shear strength that decreases to residual shear strength, whereas large shearing area tests do not develop peak shear strength—rather, the peak and residual shear strengths are the same.

Cement foam material at the laboratory-scale area of 0.006 m^2 (10 $in.^2$) exhibits elastic-brittle behavior with a peak shear strength of 0.88 MPa (128 psi) and residual strength of 0.39 MPa (56 psi). From the large-scale tests on hitched seals in the MRS with shearing area of 1.486 m^2 (2,304 $in.^2$), failure through the cement foam material occurred at a shear stress of 0.39 MPa (57 psi). At this large scale, the cement foam exhibited elastic-plastic behavior, and the peak and residual strengths are the same at 0.39 MPa (57 psi). The residual shear strength for the cement foam material appears to be similar over a large range of shearing areas, and the cement foam material no longer develops peak shear strength at large scale.

For the interfaces between cement foam and concrete blocks, both the peak and residual shear strengths exhibit scale dependence—that is, shear strength decreases with larger shear area. Peak shear strength decreases from the range of 0.71 to 0.81 MPa (103 to 117 psi) for small laboratory-scale specimens with a shearing area of about 0.006 m^2 (10 $in.^2$) to the range of 0.08 to 0.16 MPa (11 to 23 psi) for large MRS test specimens with an area of 1.486 m^2 (2,304 $in.^2$). Residual strength also decreases from about 0.27-0.29 MPa (39-42 psi) for 0.006-m^2 (10-$in.^2$) specimens to about 0.08-0.16 MPa (11-23 psi) for 1.486-m^2 (2,304-$in.^2$) specimens, as shown in Fig. 14.

Several factors could explain the scale effect in this shear

Table 6 — Summary of shear strength test results along cement foam/cement foam and cement foam/concrete block interfaces at different scales.

Property/testing scale		Cement foam material	Cement foam/concrete roof block interface	Cement foam/concrete strong floor block interface	Cement foam/concrete weak floor block interface
Peak/residual shear strength, psi	Small direct shear tests 0.006 m^2 (10 in^2)	0.88/0.39 (128/56)	0.81/0.28 (117/40)	0.8/0.29 (116/42)	0.71/0.27 (103/39)
	Large direct shear tests 0.084 m^2 (130 in^2)	not applicable	0.17/0.11 (25/16)	0.3/0.23 (44/33)	not applicable
	MRS tests 1.486 m^2 (2304 in^2)	0.39/0.39 (57/57)	0.08/0.08 (11/11)	0.16/0.16 (23/23)	0.15/0.15 (22/22)

strength data. As described earlier, the large specimens tested in the MRS developed internal heat due to the exothermic cement hydration reaction. These large specimens became warm to the touch [about 339K (150°F)] and emanated water vapor for several hours early in the cure period. This internal heating could have induced cracking within the large test specimen that could lead to a strength decrease. The internal heating phenomenon was not observed with the smaller-scale test specimens with shearing areas of 0.006 and 0.084 m^2 (10 and 130 $in.^2$). Although the cement hydration reaction still produced heat, the small specimen size enabled rapid heat dissipation, and a temperature rise was not detected. However, as seen in Fig. 14, the 0.084-m^2 (130-$in.^2$) test specimens also exhibit decreases in peak and residual strengths that are comparable in magnitude to that seen with the 1.486-m^2 (2,304-$in.^2$) test specimens. The internal heating was not seen in the 0.084-m^2 (130-$in.^2$) test specimens, and peak and residual shear strength still decreased at this scale. Thus, the internal heating experienced by the large MRS test specimens does not adequately explain the observed shear strength decrease, although it may have contributed somewhat.

The preferred explanation for the observed shear strength decrease is the non-uniform shear stress distribution across the shearing area at larger scales. The shear strength of a surface can reach high strength; however, this peak shear strength is localized and can only occur over a small area. The small laboratory specimens had shearing area of about 0.006 m^2 (10 $in.^2$) and diameter of about 76 mm (3 in.). The applied shear stress across this surface is nearly uniform. Because of the small scale and the uniform shear stress distribution across the shearing surface, the small shear area tests capture the highly localized peak shear strength before decreasing to the residual shear strength for the surface. With larger-scale tests, the applied shear stress across a failure surface is non-uniform. The shear stress is greater when closer to the load application point and decreases further away. The non-uniform shear stress across the shearing surface leads to a progressive failure across the surface. Locally with small surface area, shear failure occurs at peak shear strength; however, for the overall failure surface, shear failure occurs at average shear strength that approaches the residual shear strength of the material or the interface. Numerous research works confirm the shear strength scale effect observed in this study and verify that the shear strength converges to the residual strength of the material or interface as the test size increases (Alejano and Alonso, 2005; Bandis, 1980; Ueng et al., 2010).

To confirm the shear strength data shown in Fig. 14 on a large shearing-area scale, numerous tests on cement foam seal structures conducted at Lake Lynn Laboratory were back-analyzed to place bounds on the shear strengths of cement foam/surrounding rock interfaces. Table 7 summarizes the back-analysis results from 19 tests on 10 different structures. Most of the tests in this table were explosion tests in which a methane-air mixture was ignited to apply pressure to the test structure. The last three tests in Table 7 were hydrostatic tests in which water was pumped into a hydrostatic test chamber to apply pressure to the test structure. Most tests used cement foam having an unconfined compressive strength of about 2.41 MPa (350 psi). The rock surrounding the test seals at Lake Lynn Laboratory is limestone with a compressive strength of about 68.97 MPa (10,000 psi). From the maximum pressure on the test seal face and the seal dimensions, the maximum shear stress around the perimeter of the seal is calculated using statics. Explosion test outcomes that did not induce perceptible damage to the test seal give a lower bound estimate for the shear strength along the cement foam/rock interface. Explosion test outcomes that destroyed the seal give an upper bound estimate for the shear strength at this interface. From these explosion tests, the shear strength at the cement foam/rock interface is at least 0.21 MPa (31 psi) and up to 0.34 MPa (49 psi). However, the maximum

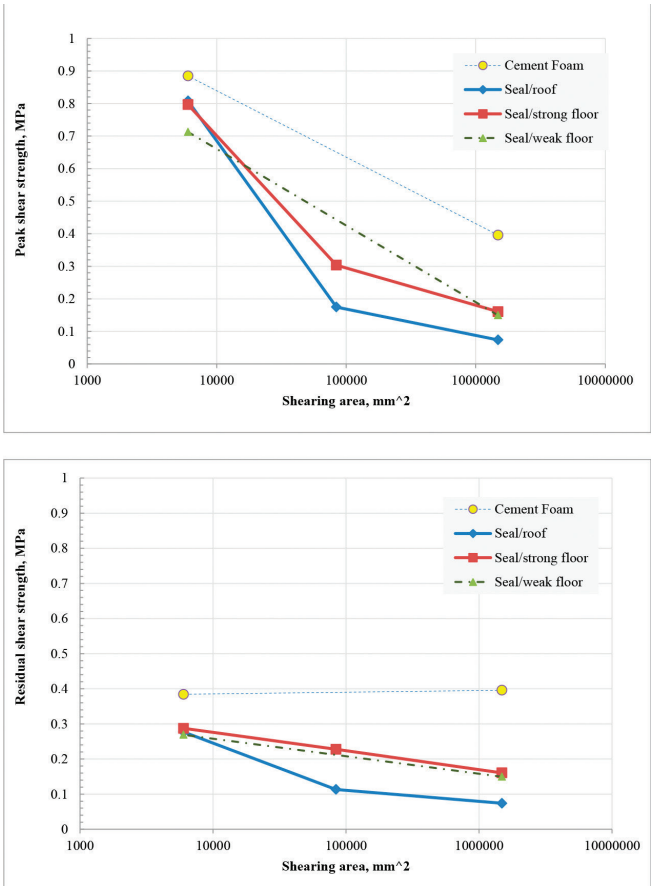

Figure 14 — Summary of average peak and residual shear strength data from 0.006-, 0.084- and 1.486-m^2 (10-, 130- and 2,304-$in.^2$) tests of cement foam/cement foam laboratory test specimens and at the cement foam/concrete block interface: cement foam material; cement foam/concrete roof block interface; cement foam/concrete strong floor block interface; cement foam/concrete weak floor block interface.

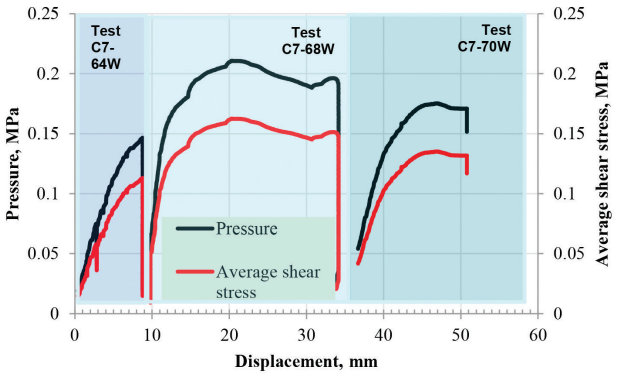

Figure 15 — Horizontal face pressure versus displacement curve and cement foam/rock interface average shear stress versus displacement curve for cement foam seal tested in hydrostatic chamber at Lake Lynn Experimental Mine.

Table 7 — Summary of cement foam/rock interface shear strength back-calculated from Lake Lynn Experimental Mine (LLEM) tests (Zipf et al., 2009).

LLEM test # and structure	W, m (ft)	H, m (ft)	T, m (ft)	Maximum face pressure, MPa (psi)	Average shear stress at perimeter, MPa (psi)	Test outcome	Reference
354 – structure 1	5.9 (19.4)	2.1 (6.90)	0.9 (3.00)	0.26 (37.9)	> 0.22 (> 32.2)	No damage	Weiss et al. (2002)
355 – structure 1	5.9 (19.4)	2.1 (6.90)	0.9 (3.00)	0.23 (32.5)	> 0.19 (>27.6)	No damage	
354 – structure 2	5.9 (19.4)	2.1 (6.90)	0.9 (2.83)	0.25 (36.0)	> 0.22 (> 32.4)	No damage	Weiss et al. (2002)
355 – structure 2	5.9 (19.4)	2.1 (6.90)	0.9 (2.83)	0.27 (38.2)	> 0.24 (> 34.4)	No damage	
354 – structure 3	5.8 (19.0)	2.3 (7.55)	0.8 (2.50)	0.21 (30.1)	> 0.22 (> 32.5)	No damage	Weiss et al. (2002)
355 – structure 3	5.8 (19.0)	2.3 (7.55)	0.8 (2.50)	0.20 (28.5)	> 0.21 (> 30.8)	No damage	
354 – structure 4	6.0 (19.7)	2.2 (7.22)	0.6 (2.00)	0.21 (30.1)	> 0.27 (> 39.8)	No damage	Weiss et al. (2002)
355 – structure 4	6.0 (19.7)	2.2 (7.22)	0.6 (2.00)	0.20 (28.5)	> 0.26 (> 37.6)	No damage	
403 – structure 5	5.8 (19.0)	2.1 (6.75)	0.8 (2.50)	0.14 (20.8)	> 0.14 (> 20.7)	No damage	Weiss et al. (2002)
404 – structure 5	5.8 (19.0)	2.1 (6.75)	0.8 (2.50)	0.20 (28.7)	> 0.20 (> 28.6)	No damage	
405 – structure 5	5.8 (19.0)	2.1 (6.75)	0.8 (2.50)	0.19 (26.7)	> 0.18 (> 26.6)	No damage	
508 – structure 6	5.7 (18.7)	2.2 (7.30)	1.6 (5.10)	0.46 (66.0)	> 0.23 (> 34.0)	No damage	Weiss and Harteis (2008)
				Average	> 0.22 (> 31.4)		
406 – structure 5	5.8 (19.0)	2.1 (6.75)	0.8 (2.50)	0.25 (35.4)	< 0.24 (< 35.3)	Destroyed	Weiss et al. (2002)
C3-44E – structure 7	6.5 (21.2)	2.7 (8.70)	1.2 (4.00)	0.22 (32.0)	< 0.17 (< 24.7)	Destroyed	Sapko et al. (2005)
L2-51E – structure 8	9.4 (30.8)	4.8 (15.6)	1.2 (4.00)	0.19 (27.5)	< 0.25 (< 35.6)	Destroyed	Sapko et al. (2005)
509 – structure 6	5.7 (18.7)	2.2 (7.30)	1.6 (5.10)	1.36 (195.5)	< 0.69 (< 100.6)	Destroyed	Weiss and Harteis (2008)
				Average	< 0.34 (< 49.0)		
C7-64W – structure 9	6.5 (21.2)	2.7 (8.70)	1.2 (4.00)	0.15 (21.0)	> 0.11 (> 16.2)	No damage	Sapko et al. (2005)
C7-68W – structure 9	6.5 (21.2)	2.7 (8.70)	1.2 (4.00)	0.21 (30.5)	0.16 (> 23.5)	No damage	
C7-70W – structure 9	6.5 (21.2)	2.7 (8.70)	1.2 (4.00)	0.17 (25.0)	0.13 (> 19.3)	No damage	
				Average	0.14 (> 19.7)		

face pressure stated in Table 7 is a short duration explosion pressure, and thus, the estimated static shear stress at the perimeter is likely an overestimate.

The last three tests in Table 7 were conducted in the hydrostatic test chamber on the same test seal, and Fig. 15 compiles the measured stress-displacement curves for each test into one relationship. As shown in Fig. 15, these tests give an estimate of the residual shear strength of about 0.14 MPa (20 psi), which is consistent with the residual shear strength data presented in Fig. 14.

Conclusions

The laboratory-scale testing and large MRS-scale testing provided extensive shear strength data on cement foam material and the interface between cement foam and concrete. Shear strength tests on the laboratory scale showed elastic-brittle behavior. The measured shear stress versus displacement curves for laboratory test specimens rise to a peak shear strength and then decrease to a residual shear strength with continued displacement. Larger-scale direct shear laboratory tests showed less brittleness behavior and the large MRS-scale tests showed elastic-plastic behavior where the peak shear strength was similar to the residual strength. For the cement foam material, the residual shear strength appears to be about 0.39 MPa (56 psi) for the material tested, and that shear strength appears to be scale-independent. For interfaces, the residual strength may be about 0.08 MPa (11 psi) along the cement foam/concrete roof block interface, and about 0.15-0.16 MPa (22-23 psi) along the cement foam/concrete floor block interface. The difference between roof and floor block shear strength probably arises due to the construction procedure, which favors better bonding along the lower (floor) interface. These shear strength values agree with the values back-calculated from the Lake Lynn Laboratory full-scale experiments (Weiss et al., 2002; Sapko et al., 2005; Weiss and Harteis, 2008).

When using an equivalent static method such as the plug formula for structural analysis of a cement foam seal, the designer should use the residual shear strength determined from small laboratory-scale tests of cement foam/concrete or rock interfaces as the best approximation for shear strength in design. That residual strength value is about 0.14 MPa (20 psi), as shown in Fig. 14.

The large MRS-scale tests of cement foam seals provided resistance functions useful for seal design using SDOF methods of analysis. A resistance function is the same as the measured applied horizontal pressure on the seal face versus horizontal displacement at seal mid-height curve as shown in Figs. 7 and 8 or 12 and 13. Figure 16 shows general resistance functions for hitched and non-hitched seals that can be used with the SDOF method of analysis for seal design. These general resistance functions are linear elastic up to about 0.14 MPa (20 psi) for non-hitched seals and 0.17 MPa (24 psi) for hitched seals. Beyond those stresses, the shear resistance increases in both cases, but at a lower rate.

Analysis of the large-scale tests in the MRS with finite element methods provided the single set of input parameters, summarized in Table 5, that replicate the observed applied face pressure versus horizontal displacement data with fidelity as shown in Figs. 12 and 13. As shown in Table 5, the best-fit shear strength values for the cement foam/concrete strong floor block are a cohesion of 0.15 MPa (22 psi) and friction coefficient of 0.5. The developed FE models can be used to calculate the resistance functions of cement foam seals with dimensions other than the ones conducted in this study.

In these large-scale tests of simulated cement foam coal mine seals, the capacity of the structure is controlled by failure along an interface between cement foam and concrete. To improve the capacity of the structure, the shear strength of the surrounding interfaces must be increased. The seal structure—whether it is a wall- or plug-like structure—requires anchorage to the surrounding rock mass. The test data reported in this study and back-analysis of other test data suggests that relying on friction along that interface may be inadequate. A designed shear connection involving rock bolts and steel reinforcement bars with embedded wire mesh may be a better solution.

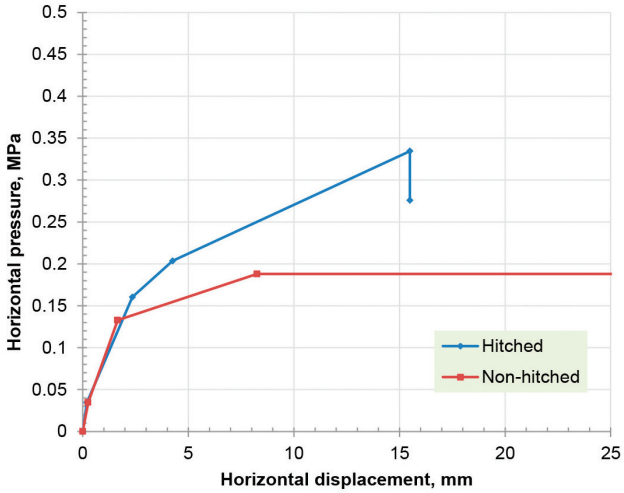

Figure 16 — Typical horizontal face pressure versus displacement relationships, also called resistance functions, for non-hitched and hitched seals.

Acknowledgments

The authors acknowledge the following colleagues whose invaluable contributions made the seal testing program possible: James Addis, Frank Karnack and Donald Sellers, physical science technicians, and Timothy Matthews, engineering technician, for assembling the testing fixture in the MRS, constructing the test seals, installing the instrumentation, and conducting the tests. The authors also acknowledge David Gearhart, electrical engineer, and Timothy Batchler, mechanical engineer, for operating the MRS and its data acquisition system.

Disclaimer

The findings and conclusions in this report are those of the authors and do not necessarily represent the views of the National Institute for Occupational Safety and Health.

References

Alejano, L.R., Alonso, E., 2005, "Considerations of the dilatancy angle in rocks and rock masses," *International Journal of Rock Mechanics and Mining Sciences*, Vol. 42, pp 481-507.

ANSYS Ver. 14.5, 2013, "Finite Element Analysis System," ANSYS, Inc., Canonsburg, Pennsylvania.

ASTM 2002, ASTM Designation E 72-02, "Standard test methods for conducting strength tests of panels for building construction," Annual Book of ASTM Standards.

Bandis, S., 1980, "Experimental Studies of Scale Effects on Shear Strength, and Deformation of Rock Joints," Ph.D. dissertation, University of Leeds.

Barnes, R.A., 2009, "Foamed concrete: application and specification," *Proceedings of the Conference on Excellence in Concrete Construction through Innovation*, Kingston University, UK, September 9-10, 2008, CRC Press, p. 3.

Chen, W.F., 2007, *Plasticity in reinforced concrete*, John Wiley and Sons, Inc., New York, NY.

Dolton, B., and Hannah, C., 2006, "Cellular Concrete: Engineering and Technological Advancement for Construction in Cold Climates," 2006 Annual General Conference of the Canadian Society for Civil Engineering, Calgary, Alberta, Canada, GC-125-1–GC-125-11.

Ehrgott, J.Q., 1973, "Investigation of the Static Uniaxial Strain and Triaxial Shear Response of Cellular Concrete," No. AEWES-MISC-PAPER-S-73-32, Army Engineer Waterways Experiment Station, Vicksburg, MS.

Final Rule 2008, Federal Register "Rules and Regulations Sealing of Abandoned Areas – Final Rule," Title 30 CFR Part 75.335 CFR, Code of Federal Regulations, Washington, DC: U.S. Government Printing Office, Office of the Federal Register 73(76), Friday, April 18, 2008, pp. 21182-21209.

Hauksdóttir, B., 2007, "Analysis of a Reinforced Concrete Shear Wall," M.Sc. Thesis, Technical University of Denmark, p. 16.

Jones, M.R., and McCarthy, A., 2006, "Heat of hydration in foamed concrete: effect of mix constituents and plastic density," *Cement and Concrete Research*, Vo. 36, No. 6, pp. 1032-1041.

Kachlakev, D.I., Miller, T., Yim, S., Chansawat, K., and Potisuk, T., 2001, "Finite Element Modeling of Reinforced Concrete Structures Strengthened with FRP Laminates," California Polytechnic State University, San Luis Obispo, CA, and Oregon State University, Corvallis, OR, for Oregon Department of Transportation, May.

Krieg, R.D., 1972, "A Simple Constitutive Description for Cellular Concrete," Sandia National Laboratories, SC-DR-72-0883.

Lee, M.Y., Bronowski, D.R., and Hardy, R.D., 2004, "Laboratory Constitutive Characterization of Cellular Concrete," Sandia National Laboratories, SAND2004-1030.

Mohamed, K.M., Zipf, R.K., Gearhart, D.F., and Batchler, T.J., 2013, "Experimental and analytical validation of plain and reinforced concrete mine seal designs," *Society for Mining, Metallurgy and Exploration Transactions*, Vol. 334, pp. 477-488.

Othuman, M.A., and Wang, Y.C., 2011, "An experimental investigation of mechanical properties of lightweight foamed concrete subjected to elevated temperatures up to 600°C," *Concrete Research Letters*, Vol. 1, No. 4, pp. 142-157.

Richway Industries, 2013, http://www.cretefoamer.com, accessed June 2013.

Sapko M.J., Weiss E.S., and Harteis, S.P., 2005, "Methods for evaluating explosion resistant ventilation structures," *Proceedings of the 8th International Mine Ventilation Congress*, Australasian Institute of Mining and Metallurgy, Victoria, Australia, pp. 211-219.

Slawson T.R., 1995, "Wall Response to Airblast Loads: The Wall Analysis Code (WAC)," prepared for the U.S. Army ERDC, Vicksburg, MS, Contract DACA39-95-C-0009, ARA-TR-95-5208, November 1995.

Ueng, T.S., Jou, Y.J., and Peng, I.H., 2010, "Scale effect on shear strength of computer-aided-manufactured joints," *Journal of Geo Engineering*, Vol. 5, No. 2, pp. 29-37.

UFC 3-340-02 2008, "Unified Facilities Criteria (UFC): Structures to Resist the Effects of Accidental Explosions," Department of Defense, United States of America, 1943 pp., http://www.wbdg.org/ccb/DOD/UFC/ufc_3_340_02_pdf.pdf, accessed June 2013.

Vasudevan, G., and Kothandaraman S., 2011, "Parametric study on nonlinear finite element analysis on flexural behavior of RC Beams using ANSYS," *International Journal of Civil and Structural Engineering*, Vol. 2, No. 1.

Weiss E.S., Cashdollar K.L., Sapko M.J., 2002, "Evaluation of explosion resistant seals, stoppings, and overcasts for ventilation control in underground coal mining," U.S. Department of Health and Human Services, National Institute for Occupational Safety and Health, Pittsburgh Research Laboratory, RI 9659, 48 pp.

Weiss, E.S., Harteis, S.P. 2008, "Strengthening existing 20-psi mine ventilation seals with carbon fiber-reinforced polymer reinforcement," U.S. Department of Health and Human Services, National Institute for Occupational Safety and Health, Pittsburgh Research Laboratory, RI 9673, 38 pp.

Wolanski, A.J., 2004, "Flexural behavior of reinforced and pre stressed concrete beams using finite element analysis," M.Sc. Thesis, Marquette University, p. 28.

Zipf, R.K., Weiss, E.S., Harteis, S.P., and Sapko, M.J., 2009, "Compendium of structural testing data for 20-psi coal mine seals," IC9515, U.S. Dept. of Health and Human Services, National Institute for Occupational Safety and Health, 143 pp.

Zipf, R.K., Mohamed, K.M., and McMahon, G.W., 2009, "Design and analysis of a new method to test mine seals," *Proceedings of 80th Shock and Vibration Symposium*, San Diego, CA, 17 pp.